Available online at www.sciencedirect.com
SCIENCE DIRECT®
Cement & Concrete Composites 27 (2005) 503–514
Cement & Concrete Composites
www.elsevier.com/locate/cemconcomp

An analytical model for crack control in reinforced concrete elements under combined forces

Vincenzo Colotti, Giuseppe Spadea *

Department of Structural Engineering, University of Calabria, Rende (Cosenza), Italy

Received 23 December 2003; accepted 13 July 2004

Abstract

A rational model for design with crack control of reinforced concrete structures is presented. The model, based on the *Softened Truss Theory*, allows crack width in reinforced concrete elements under combined axial, flexure, shear and torsion forces to be determined. By calculating the corresponding principal tensile strains, normalized with respect to an appropriate reference value, and by assuming suitable stress–strain relationships, the equilibrium and compatibility conditions are imposed. Thus an appropriate iterative procedure allows strain contour as well as cracking width to be determined. The results obtained are presented in graphs to ease practical and design applications.

Keywords: Axial load; Bending; Crack control; Reinforced concrete structures; Shear; Softened truss theory

1. Introduction

Crack control of reinforced concrete (RC) structures is fundamental for serviceability and durability. In fact, crack opening leads to the corrosion of steel reinforcement and the overall cracking pattern affects the rigidity, ductility and energy absorption capacity of structural elements. Therefore feasible, clear and simple design rules regarding cracking in reinforced concrete structures are important for practising professionals.

An efficient control of cracking requires refined analytical modeling capable of accurately predicting crack width and crack spacing under different load conditions. Given the complexity of the problem, many authors have proposed semi-empirical methods to evaluate the crack width of reinforced concrete elements [1,5,7,11,13,17]. These methods are not generally applicable, as they are limited to simple geometries and loading conditions (in practice, for members subjected to flexure or axial tension).

Current procedures consider uniaxial strain conditions as in the CEB-FIP Model Code [2] which defines the average crack width under normal stresses as the product of the average strain of steel rebars and the average crack spacing between two consecutive cracks. This formulation is directly applicable when the principal tensile strain direction is coincident with the bar direction (members under axial force or pure bending). Semi-empirical formulations, based on experimental evidence, have been proposed [11] for axial or pure bending forces. On the other hand, analogous formulations, suitable for reasonably predicting the average principal tensile strain and the crack opening in the case of combined forces (axial force and/or bending combined with shear and/or torsion), are not yet available.

In this paper an analytical method, based on the application of the *Softened Truss Theory* [8] which is capable of describing the crack pattern of (RC) elements under combined forces, is presented. A uniformly

* Corresponding author. Fax: +39 0984 494045.
E-mail address: g.spadea@unical.it (G. Spadea).

0958-9465/$ - see front matter © 2004 Elsevier Ltd. All rights reserved.
doi:10.1016/j.cemconcomp.2004.09.002

Nomenclature

A_l	area of longitudinal tension reinforcement
A_0	area enclosed by the shear flow
A_t	area of shear reinforcement within a distance s_t
b	beam width
c	concrete cover
c'	distance from outer edge of section and internal edge of stirrups
d	effective depth
E_c	modulus of elasticity of concrete
E_s	modulus of elasticity of steel
f_c	concrete compressive cylinder strength
f_{cr}	concrete cracking stress
f_l, f_t	stress in the longitudinal and transverse reinforcement, respectively
f_y	yield stress of steel
G	dead load
h	beam height
h_m	height of equivalent web panel
h^*	internal lever arm
k	$\rho_l E_s \varepsilon_0 / f_c$
k_1	coefficient for bonding property of bars
k_2	coefficient for deformation diagram form
L	beam length
M	flexural moment
M_t	torsional moment
n	modular ratio
Q	live load
r	parameter relative to concrete in tension
s_l, s_t	bar spacing in the l and t direction, respectively
s_{rm}	average crack spacing
T	tension force
t_d	thickness of the shear flow zone
u	ρ_t / ρ_l
V	shear force
w_a	admissible (limit) crack width
w_k	design crack width
w_m	average crack width
x_c	depth of the neutral axis
α	angle between the l–t coordinate system and the principal directions d–r
β	f_{cr}/f_c
β_0	coefficient that correlates the average crack width to the design value
β_1	coefficient characterizing the bond quality of bars
β_2	coefficient representing the influence of the duration of loading
ε_{cr}	concrete cracking strain
ε_d	average principal strain in the d direction
$\varepsilon_l, \varepsilon_t, \gamma_{lt}$	strains in (l–t)-coordinate system
$\varepsilon_{ly}, \varepsilon_{ty}$	yield strain of longitudinal and transverse reinforcement, respectively
ε_0	strain in concrete at peak stress f_c
ε_r	average principal strain in the r direction
ε_{rm}	average steel strain within s_{rm} spacing
ζ	softening factor
ρ_l, ρ_t	longitudinal and transverse reinforcement ratio, respectively
ρ_r	ratio of the area of tensile reinforcement to the effective tension area, bh_m
σ^*, τ^*	normalized stresses
σ_d	principal stress in the d direction
$\sigma_l, \sigma_t, \tau_{lt}$	stresses in (l–t)-coordinate system
σ_r	principal stress in the r direction
σ_s	stress in the reinforcement at the cracked section under service load
σ_{sr}	stress in the reinforcement at the cracked section under load that causes cracking
ϕ	bar diameter
ψ_1	load combination factor

loaded panel, under normal and shear stresses, is analyzed. Compatibility and equilibrium equations and stress–strain relationships of materials allow, for given load conditions, the average principal tensile strain, which plays a fundamental role in the evaluation of crack width, to be determined.

2. Formulation

Consider a reinforced concrete panel of constant thickness subject to a uniform stress; orthogonal steel rebars have constant spacing in each direction (Fig. 1). From a mechanistic point of view, the panel can be represented as a set of uniaxial elements which describe, respectively, the average behaviour of the steel rebars and the concrete. There are many structural elements like this, such as thin webs of beams, shear walls and low curvature shells.

The behaviour of concrete under a biaxial state of stress can be described by a unidimensional approach. It is based on the assumption of equivalent uniaxial stress–strain relationships corresponding, respectively, to the principal strain directions.

From basic mechanical considerations, the following assumptions for equilibrium, compatibility and stress–strain relationships are made:

- average stresses and strains are assumed for a significant area of the panel;

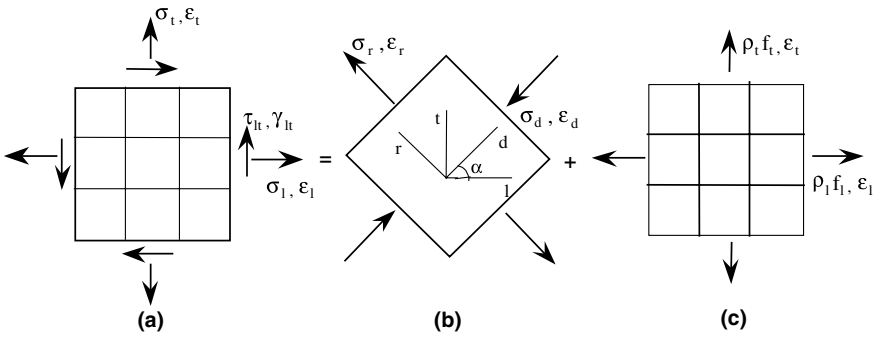

Fig. 1. Panel scheme: (a) RC membrane element, (b) concrete element and (c) steel reinforcement.

- the concrete behaviour is described by the principal compression and tensile stresses;
- stress and strain principal directions in concrete are coincident;
- concrete cracks are orthogonal to tensile strain direction;
- steel rebars resist axial force in their own direction only.

The following equilibrium equations can then be written (Fig. 1b):

$$\sigma_l = \sigma_r \sin^2\alpha - \sigma_d \cos^2\alpha + \rho_l f_l \tag{1a}$$

$$\sigma_t = \sigma_r \cos^2\alpha - \sigma_d \sin^2\alpha + \rho_t f_t \tag{1b}$$

$$\tau_{lt} = (\sigma_r + \sigma_d)\sin\alpha\cos\alpha \tag{1c}$$

where σ_l and σ_t are the normal stresses in the l- and t-directions, respectively; σ_d and σ_r, the principal stresses in the d- and r-directions, respectively; τ_{lt}, the shear stress in the l–t coordinate system; ρ_l and ρ_t, are smeared longitudinal and transverse reinforcement ratio, respectively; f_l and f_t, the stresses in the smeared longitudinal and transverse reinforcement, respectively and α is the angle between the l and t coordinate system and the principal directions d–r.

The compatibility equations for strains are given by

$$\varepsilon_l = \varepsilon_r \sin^2\alpha - \varepsilon_d \cos^2\alpha \tag{2a}$$

$$\varepsilon_t = \varepsilon_r \cos^2\alpha - \varepsilon_d \sin^2\alpha \tag{2b}$$

$$\gamma_{lt} = 2(\varepsilon_r + \varepsilon_d)\sin\alpha\cos\alpha \tag{2c}$$

with

$$\tan 2\alpha = \gamma_{lt}/(\varepsilon_l - \varepsilon_t) \tag{3}$$

where ε_l and ε_t are the average strains in the l- and t-directions, respectively; ε_d and ε_r, the average principal strains in the d- and r-directions, respectively and γ_{lt} is the average shear strain in the l–t coordinate system.

The assumed stress strain relationships for concrete are those proposed by Hsu [8], which take into account the main phenomena related to biaxial stress states (in terms of strength and strain softening effect) and the presence of embedded steel rebars (considering the tension stiffening effect). In particular, for compression concrete, the principal compressive stress σ_d is related to the principal tensile and compressive strains ε_r and ε_d as follows (Fig. 2a):

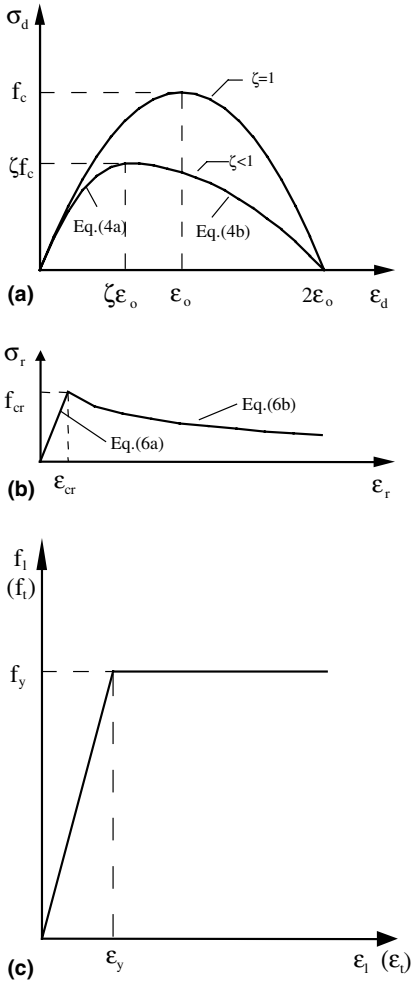

Fig. 2. Stress–strain relationships: (a) concrete in compression; (b) concrete in tension; (c) steel rebars.

(a) *ascending branch*: $\frac{\varepsilon_d}{\zeta\varepsilon_0} \leqslant 1$

$$\sigma_d = \zeta f_c \left[2\left(\frac{\varepsilon_d}{\zeta\varepsilon_0}\right) - \left(\frac{\varepsilon_d}{\zeta\varepsilon_0}\right)^2 \right] \tag{4a}$$

(b) *descending branch*: $\frac{\varepsilon_d}{\zeta\varepsilon_0} > 1$

$$\sigma_d = \zeta f_c \left[1 - \left(\frac{\frac{\varepsilon_d}{\zeta\varepsilon_0} - 1}{\frac{2}{\zeta} - 1} \right)^2 \right] \tag{4b}$$

where f_c is the concrete compressive cylinder strength and ε_0 the strain at the peak stress f_c; ζ the softening factor.

The coefficient ζ takes into account the degradation phenomenon consequent to the diagonal cracking (biaxial softening). The following relation is assumed for ζ [8]:

$$\zeta = \frac{0.9}{\sqrt{1 + 600\varepsilon_r}} \tag{5}$$

The following formulae are adopted for tensile concrete stress–strain relationships:

(a) *ascending branch*: $\varepsilon_r \leqslant \varepsilon_{cr}$

$$\sigma_r = f_{cr}\left(\frac{\varepsilon_r}{\varepsilon_{cr}}\right) \tag{6a}$$

(b) *descending branch*: $\varepsilon_r > \varepsilon_{cr}$

$$\sigma_r = f_{cr}\left(\frac{\varepsilon_{cr}}{\varepsilon_r}\right)^{0.4} \tag{6b}$$

where f_{cr} is the concrete cracking stress; ε_{cr} the concrete cracking strain. Note that Eq. (6b), which relates to the post-cracking stage, also takes into account the tension stiffening effect. The stress–strain relationships of Eqs. (4) and (6) are shown in Figs. 2a and b, respectively.

A typical bilinear elasto-plastic behaviour is assumed for steel, as shown in Fig. 2c. However, in the present study, which aims to analyze cracking in the serviceability state, it is appropriate to consider the initial elastic slope only, and not the plastic branch. Therefore, to describe the actual behaviour of the steel a typical linear relationship can be considered:

$$f_l = E_s\varepsilon_l \qquad \text{for} \quad \varepsilon_l \leqslant \varepsilon_{ly} \tag{7a}$$

$$f_t = E_s\varepsilon_t \qquad \text{for} \quad \varepsilon_t \leqslant \varepsilon_{ty} \tag{7b}$$

where E_s is the modulus of elasticity of steel and ε_{ly} and ε_{ty} are the strains corresponding to the elastic limit of the rebar positioned in the l and t directions, respectively.

3. Solution method

The model described in the preceding section can be used to determine the crack pattern and crack width of (RC) elements. Due to the nonlinearity of the problem, it is necessary to develop a procedure, which in turn permits the calculation of the main variables that regulate the occurrence of cracking.

The model solution is governed by the equilibrium equation (1), compatibility conditions (2) and by the stress–strain relationships (4), (6) and (7). At any given load, there is a corresponding panel deformation. The stresses that produce such deformations are obtained by solving the equations cited previously.

However, when all the panel loading components are known, the calculation of the corresponding deformations cannot be obtained directly (in an explicit manner), and the solution must be found by means of an iterative procedure. In this procedure, the calculation of the deformed state of a membrane element, starting from known values of the tension components, is necessary.

In the following a mixed procedure, where some tension and deformation components are assumed in order to facilitate the calculation of the remaining variables, is presented. Such a procedure can be advantageously utilized to solve the problem by means of dimensionless equations, thus permitting simplification, generalization and an effective graphic presentation of the results obtained.

Initially, a plane stress state is assumed, characterized by a known normal stress in the transverse direction (in particular, $\sigma_t = 0$). Such a stress state is typical of many structural elements where a cracking condition is bound to occur (beam webs, elements of thin walls, etc.).

Having set the initial parameters in terms of geometry and material properties and, moreover, given tensile strains ε_r and inclination angle of cracks α, the remaining unknown values of stress and strain are obtained. Hence it becomes possible to relate the tension components σ_l and τ_{lt} to the tensile principal strain ε_r, which, as will be seen later, represents the main variable in tackling the problem of cracking in (RC) elements.

From an analytical point of view the procedure is as follows.

From Eq. (1b), and taking into account Eqs. (2b) and (7b) it follows:

$$\sigma_t = \sin^2\alpha(-\sigma_d - \rho_t E_s\varepsilon_d) + \cos^2\alpha(\sigma_r + \rho_t E_s\varepsilon_r) = 0 \tag{8}$$

Substituting the tension and compression relationships for concrete in Eq. (8), the following relationships can be obtained:

(a) *ascending branch*: $\frac{\varepsilon_d}{\zeta\varepsilon_0} \leqslant 1$

$$\sin^2\alpha\left[\frac{f_c}{\zeta\varepsilon_0^2}\varepsilon_d^2 - \left(\frac{2f_c}{\varepsilon_0} + \rho_t E_s\right)\varepsilon_d\right] + \cos^2\alpha[f_{cr}r_{(\varepsilon_r)} + \rho_t E_s\varepsilon_r] = 0 \tag{9}$$

where

$$r_{(\varepsilon_r)} = \frac{\varepsilon_r}{\varepsilon_{cr}} \qquad \text{for} \quad \varepsilon_r \leqslant \varepsilon_{cr} \tag{10a}$$

$$r_{(\varepsilon_r)} = \left(\frac{\varepsilon_{cr}}{\varepsilon_r}\right)^{0.4} \qquad \text{for} \quad \varepsilon_r > \varepsilon_{cr} \tag{10b}$$

In Eq. (9) the only unknown is ε_d. The following terms are introduced:

$$\beta = \frac{f_{cr}}{f_c}; \quad u = \frac{\rho_t}{\rho_l}; \quad k = \frac{\rho_l E_s \varepsilon_0}{f_c} \tag{11}$$

and, by reorganizing the terms and solving:

$$\left(\frac{\varepsilon_d}{\varepsilon_0}\right)^2 - 2\zeta\left(1+\frac{uk}{2}\right)\frac{\varepsilon_d}{\varepsilon_0} + \zeta\cot^2\alpha\left(\beta r_{(\varepsilon_r)} + uk\frac{\varepsilon_r}{\varepsilon_0}\right) = 0 \tag{12}$$

the following solution in terms of the relative principal strain is obtained:

$$\frac{\varepsilon_d}{\varepsilon_0} = \zeta\left(1+\frac{uk}{2}\right) - \sqrt{\zeta^2\left(1+\frac{uk}{2}\right)^2 - \zeta\cot^2\alpha\left(\beta r_{(\varepsilon_r)} + uk\frac{\varepsilon_r}{\varepsilon_0}\right)} \tag{13}$$

(b) *descending branch*: $\frac{\varepsilon_d}{\zeta\varepsilon_0} > 1$

$$\sin^2\alpha\left[\frac{-4\zeta(1-\zeta)}{(2-\zeta)^2}f_c - \frac{2\zeta^2}{(2-\zeta)^2}f_c\frac{\varepsilon_d}{\varepsilon_0} + \frac{\zeta}{(2-\zeta)^2}f_c\left(\frac{\varepsilon_d}{\varepsilon_0}\right)^2 - \rho_t E_s \varepsilon_d\right] + \cos^2\alpha[f_{cr} r_{(\varepsilon_r)} + \rho_t E_s \varepsilon_r] = 0 \tag{14}$$

Using the terms shown in Eq. (11), and by reorganizing the terms with respect to ε_d, it can be shown that:

$$\left(\frac{\varepsilon_d}{\varepsilon_0}\right)^2 - 2\left[\zeta + \frac{uk}{2}\frac{(2-\zeta)^2}{\zeta}\right]\frac{\varepsilon_d}{\varepsilon_0} + \frac{(2-\zeta)^2}{\zeta}\cot^2\alpha\left(\beta r_{(\varepsilon_r)} + uk\frac{\varepsilon_r}{\varepsilon_0}\right) - 4(1-\zeta) = 0 \tag{15}$$

from which the following solution in terms of relative principal strain is obtained:

$$\frac{\varepsilon_d}{\varepsilon_0} = \zeta + \frac{(2-\zeta)^2}{2\zeta}uk - \sqrt{\left[\zeta + \frac{(2-\zeta)^2}{2\zeta}uk\right]^2 - \frac{(2-\zeta)^2}{\zeta}\cot^2\alpha\left(\beta r_{(\varepsilon_r)} + uk\frac{\varepsilon_r}{\varepsilon_0}\right) + 4(1-\zeta)} \tag{16}$$

Once the principal compressive strain, ε_d, is obtained, the tensile stress, with regard to the l–t reference frame, can be found by using the equilibrium equations and the previous assumptions. Therefore:

(a) *ascending branch*: $\frac{\varepsilon_d}{\zeta\varepsilon_0} \leqslant 1$

$$\sigma^* = \frac{\sigma_l}{f_c} = \cos^2\alpha\left[\frac{1}{\zeta}\left(\frac{\varepsilon_d}{\varepsilon_0}\right)^2 - (2+k)\frac{\varepsilon_d}{\varepsilon_0}\right] + \sin^2\alpha\left[\beta r_{(\varepsilon_r)} + k\frac{\varepsilon_r}{\varepsilon_0}\right] \tag{17a}$$

$$\tau^* = \frac{\tau_{lt}}{f_c} = \sin\alpha\cos\alpha\left[2\frac{\varepsilon_d}{\varepsilon} - \frac{1}{\zeta}\left(\frac{\varepsilon_d}{\varepsilon_0}\right)^2 + \beta r_{(\varepsilon_r)}\right] \tag{17b}$$

(b) *descending branch*: $\frac{\varepsilon_d}{\zeta\varepsilon_0} > 1$

$$\sigma^* = \frac{\sigma_l}{f_c} = \cos^2\alpha\left[\frac{\zeta}{(2-\zeta)^2}\left(\frac{\varepsilon_d}{\varepsilon_0}\right)^2 - \left(k + \frac{2\zeta^2}{(2-\zeta)^2}\right)\frac{\varepsilon_d}{\varepsilon_0} - \frac{4\zeta(1-\zeta)}{(2-\zeta)^2}\right] + \sin^2\alpha\left[\beta r_{(\varepsilon_r)} + k\frac{\varepsilon_r}{\varepsilon_0}\right] \tag{18a}$$

$$\tau^* = \frac{\tau_{lt}}{f_c} = \sin\alpha\cos\alpha\left\{\frac{\zeta}{(2-\zeta)^2}\left[4(1-\zeta) + 2\zeta\frac{\varepsilon_d}{\varepsilon_0} - \left(\frac{\varepsilon_d}{\varepsilon_0}\right)^2\right] + \beta r_{(\varepsilon_r)}\right\} \tag{18b}$$

By solving the equations above, suitable graphs that show the relationship between the normalized axial stress, σ^*, and the normalized shear stress, τ^*, for different values of ρ_t/ρ_l, $\varepsilon_r/\varepsilon_0$, and k, can be developed (see Appendix A). These graphs are only applicable for plane stress states at which $\sigma_t = 0$ and to solve problems of crack-control.

4. Application of the model to beams

In the preceding sections a procedure for relating the principal tensile strain ε_r to the plane stress state in analyzing (RC) membrane elements has been presented. In the case of a uniaxial element (beam), an equivalent idealized membrane element have to be defined. Therefore from the web of the beam the tension area (ideal tension stringer) have to be extrapolated, which can be considered equivalent to a plate subjected to normal tension, with or without shear stress components. In this paper, the formulation proposed by Oh and Kang [13], based on an energy approach, has been referred to in interpreting the geometry of such an element.

In particular, by assuming that the strain energy of the concrete area below the neutral axis of the cross-section of the beam, is equal to the strain energy of an equivalent area where the deformation is assumed to be uniform and equal to the actual deformation of steel in tension, the height (h_m) of the equivalent web panel (or ideal stringer) is given by the following relation (Fig. 3a):

$$h_m = \frac{(h-x_c)^3}{3(d-x_c)^2} \tag{19}$$

where h, d and x_c are the total height, the effective depth and the depth of the neutral axis, respectively.

Once the geometry of the equivalent membrane element has been defined and the principal tensile strain fixed, it is only necessary to calculate the average

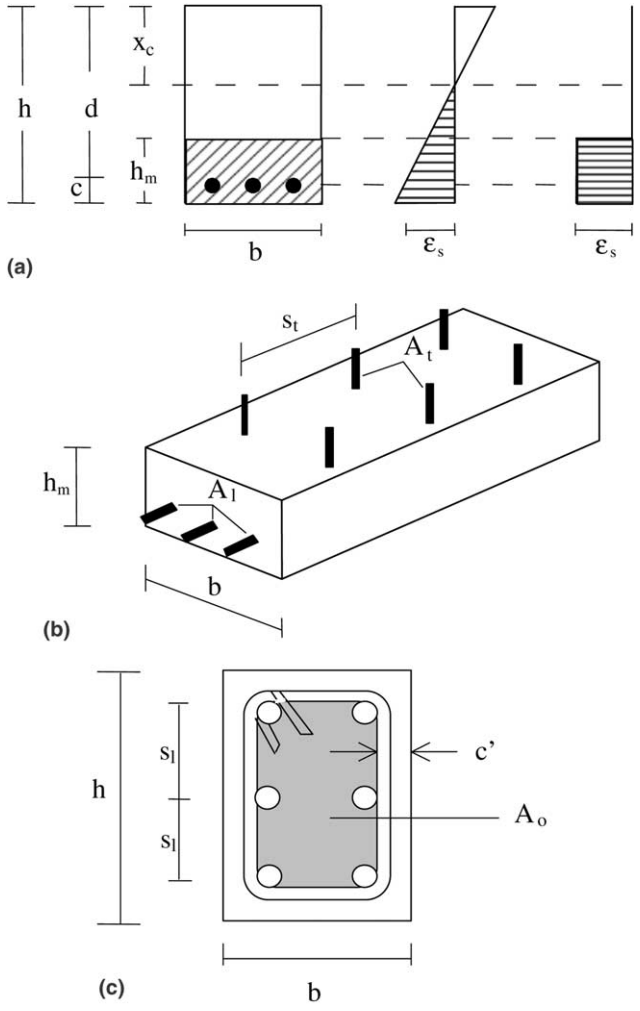

Fig. 3. Geometric values of an equivalent panel strip in an RC beam: (a) equivalent height h_m; (b) equivalent web panel; (c) cross-section for torsion.

spacing of the cracks to complete the solution of the cracking problem.

However, it should be noted that, given that this parameter is influenced by several factors, which make its true value rather uncertain, the use of formulae based on semi-empirical static analysis of experimental results is acceptable in design practice.

In this approach, the following relations to obtain the average crack spacing are useful:

- for elements subjected mainly to bending or tension, according to the current formula proposed by Eurocode 2 [6]:

$$s_{rm} = 50 + 0.25 k_1 k_2 \frac{\phi}{\rho_r} \tag{20}$$

where ϕ is the bar diameter in mm; k_1 is a coefficient that takes into account the bonding property of the bars ($k_1 = 1.6$ for smooth bars, $k_1 = 0.8$ for deformed bars); k_2 is a coefficient that takes into account the form of the deformation diagrams ($k_2 = 0.5$ for bending, $k_2 = 1.0$ for pure tension); ρ_r is the ratio of steel reinforcement to the effective tension area, bh_m, as shown in Fig. 3a;

- for elements subjected to combined action of bending, shear and/or torsion [10]:

$$\begin{aligned} s_{rm} &= s_l \quad \text{for } \frac{s_l}{s_t} < 0.55 \\ s_{rm} &= \frac{s_l + s_t}{2\sqrt{2}} \quad \text{for } 0.55 \leqslant \frac{s_l}{s_t} < 1.80 \\ s_{rm} &= s_t \quad \text{for } \frac{s_l}{s_t} > 1.80 \end{aligned} \tag{21}$$

where s_l and s_t are the center-to-center bar spacing in the l and t directions, respectively. If the longitudinal rebars are concentrated at the top or bottom level of the cross-section (i.e. the longitudinal rebars of a beam in bending), s_l in Eq. (21) is replaced by the value of the spacing found by Eq. (20).

5. Comparison with experimental results

To verify the accuracy of the proposed model in predicting crack width in (RC) elements, a numerical investigation with respect to a number of beams for which the experimental results are available in the literature [5,12,14–16,18] has been made.

In Table 1 the main mechanical and geometric properties of the beams analyzed are shown. The series of comparisons refer to (RC) beams tested in bending, bending and shear as well as in torsion. In Figs. 4–9 the experimental results and the analytical results based on the applied load–crack width relationship, are compared.

In the same figures, the curves obtained using the formulae of Eurocode 2 [6] are also shown. These formulae, only valid for members subjected to bending and/or axial force, can be synthesized as follows:

$$w_m = s_{rm} \varepsilon_{rm} \tag{22a}$$

$$w_k = \beta_0 w_m \tag{22b}$$

with

$$\varepsilon_{rm} = \frac{\sigma_s}{E_s}\left[1 - \beta_1 \beta_2 \left(\frac{\sigma_{sr}}{\sigma_s}\right)^2\right] \tag{23}$$

where w_m is the average crack width; w_k is the design crack width; β_0 is a coefficient that correlates the average crack width to the design value, which can be assumed equal to 1.7; s_{rm} is the average crack spacing whose expression is given by Eq. (20); ε_{rm} is the average steel strain within the s_{rm} spacing; σ_s is the stress in the longitudinal steel calculated in the cracked section; σ_{sr} is the

Table 1
Main properties of analyzed beams

Ref.	Beam label	f_c (MPa)	b (mm)	h (mm)	A_l (Ø mm)	Loading regime
Desayi and Rao [5]	KB1	33.1	200	350	2Ø16	Bending
	KB2	40.4	200	350	4Ø12	Bending
Makhlouf and Malhas [12]	G1	40	600	400	4Ø14 2Ø20	Bending
	G2	40	600	400	6Ø20	Bending
Tan et al. [16]	TS	43.5	200	500	4Ø13	Bending
Rahal and Collins [14]	RC1-2	52.3	300	600	9Ø25	Bending shear
	RC2-2	38.2	340	640	10Ø25	Bending shear
Yoon et al. [18]	M1-N	67	375	750	10Ø30	Bending shear
	M2-S	67	375	750	10Ø30	Bending shear
Rasmussen and Baker [15]	B30.3	36.3	160	275	2Ø18	Torsion
	B50.3	61.7	160	275	2Ø18	Torsion

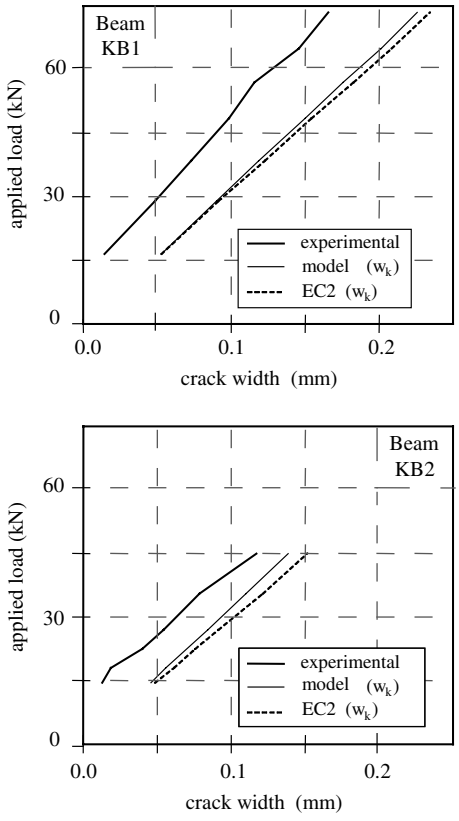

Fig. 4. Comparison between experimental and numerical results for beams tested by Desayi and Rao [5].

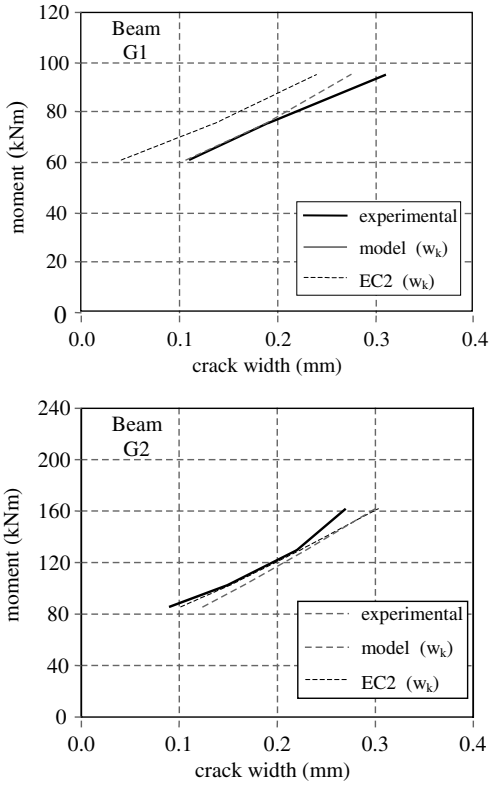

Fig. 5. Comparison between experimental and numerical results for beams tested by Makhlouf and Malhas [12].

stress in the longitudinal steel calculated under load that causes cracking of the section; β_1 and β_2 are coefficients that take into account the bonding property of the bars ($\beta_1 = 1$ for high bond bars; $\beta_1 = 0.5$ for smooth bars) and the nature of the load ($\beta_2 = 1$ for first loading; $\beta_2 = 0{,}5$ for long term load or for a large number of cycles of loads), respectively.

To obtain the analytical results, an iterative procedure [4], based on the classical Newton–Raphson method, has been utilized to solve the governing equations in terms of load–deformation curve. The crack-width reported, indicated in Figs. 4–9 with w_m or w_k, are evaluated by the relations: $w_m = s_{rm}\varepsilon_r$, $w_k = \beta_0 w_m$, with $\beta_0 = 1.7$, s_{rm} given by Eq. (20) or (21), and ε_r resulting from the solution of Eqs. (1)–(7). Furthermore, the following assumptions are made: $f_{cr} = 0.31\ f_c^{0.5}$ (in MPa); $\varepsilon_{cr} = 0.00008$, as suggested by Hsu [8].

An analysis of these figures confirms that the proposed model gives results that are in general agreement with the experimental ones. Some results show a slight over-estimation of the crack-widths, while a minor part

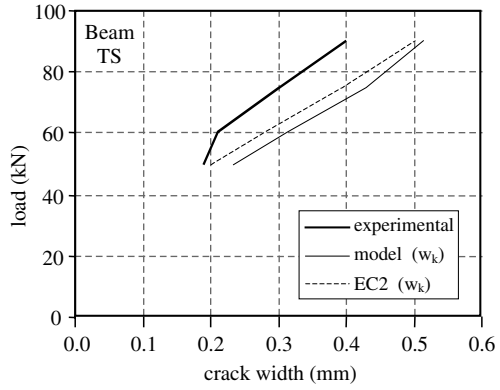

Fig. 6. Comparison between experimental and numerical results for beams tested by Tan et al. [16].

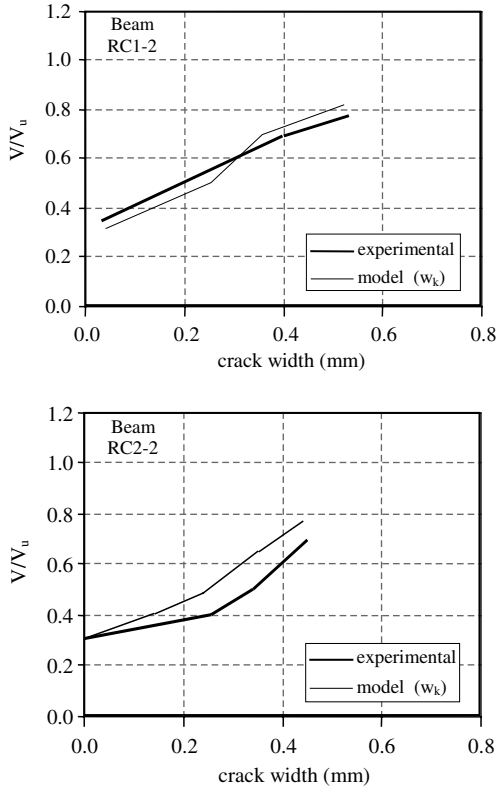

Fig. 7. Comparison between experimental and numerical results for beams tested by Rahal and Collins [14].

of them show a slight under-estimation of the crack-widths and hence the model appears to be rather conservative. A good correlation is also observed between the results obtained with this model and the ones found in the Eurocode 2 [6] for bending, as shown in Figs. 4–6.

With reference to the beams tested by Rasmussen and Baker [15] under torsion, the application of the model requires that the thickness t_d of the resisting annular section has to be determined, in order to evaluate the flow

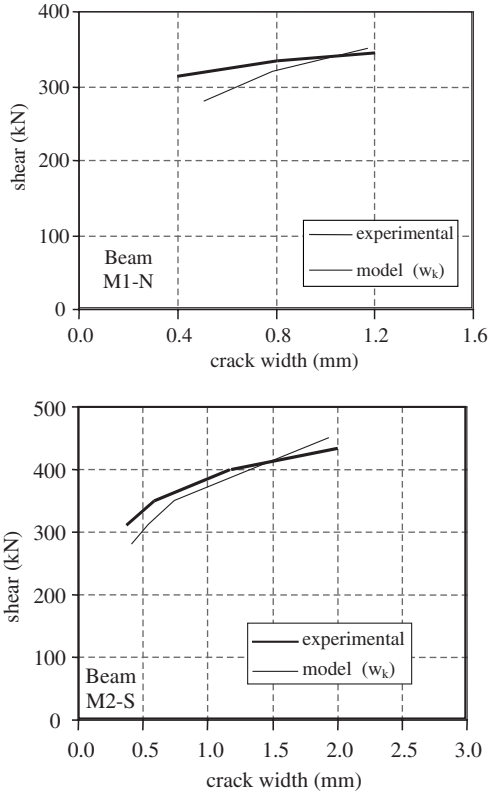

Fig. 8. Comparison between experimental and numerical results for beams tested by Yoon et al. [18].

of the shear stresses produced by the torsional load. Hence, the following relation [9] has been used:

$$t_d = 2c' \tag{24}$$

where c' represents the distance from the outer edge of the cross-section to the interior edge of the stirrups (Fig. 3c). In fact the condition expressed by Eq. (24) is the same as the average line of the steel cage formed by the stirrups and the longitudinal bars, which coincides with the average value of the circulating flow of shear stresses resulting from the torsional action. If the value of the external torsional moment M_t is known and the thickness of resisting annular section t_d is fixed, the shear stress τ_{lt} can be obtained by means of the well known Bredt formula:

$$\tau_{lt} = \frac{M_t}{2A_0 t_d} \tag{25}$$

where A_0 represents the area enclosed by the average value of the shear flow (Fig. 3c).

Then, in Fig. 9 the analytical and experimental results for beams B30.3 and B50.3 are shown in terms of torsional moment-crack width relationship. As can be seen, even for torsional diagonal (inclined) cracks the correlation between analytical and experimental curves is quite

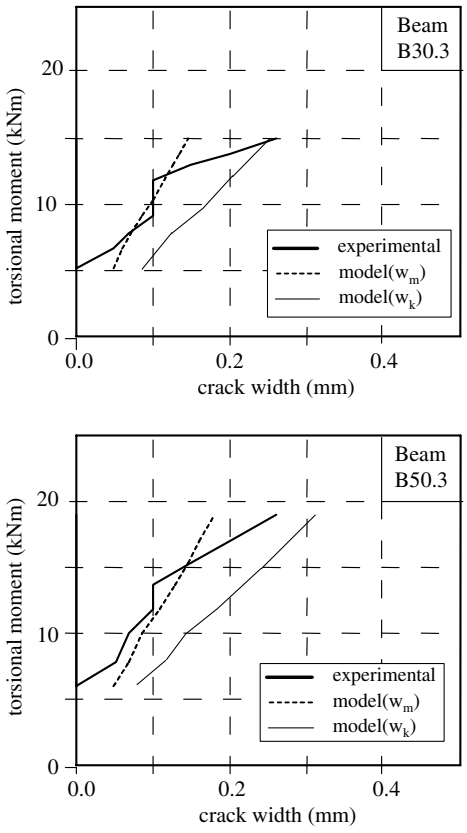

Fig. 9. Comparison between experimental and numerical results for beams tested by Rasmussen and and Baker [15].

satisfactory, particularly for torsional loads well below the ultimate capacity, i.e. in the serviceability limit state.

6. Cracking diagrams and numerical application

The procedure described above allows us to obtain simple graphs which in turn can be used to verify the cracking membrane element, subjected to a given tensile stress [3]. Once the values that are to be assigned to the principal tensile strain (normalized with respect to a reference value, for example $\varepsilon_0 = 0.002$) and the value of dimensionless parameters u and k are fixed, the graphs shown in Appendix A can be drawn.

For design purposes the use of such graphs is analogous to the corresponding design charts for section under compression-bending for conditions relative to limit-state-design. Numerical applications and details of how to better utilize these are given in Appendix B.

7. Conclusions

An innovative approach for the control of cracking in (RC) elements subject to plane stress states has been proposed. A scheme of the membrane element has been presented, and it has been shown how this can be utilized to investigate structures that are highly susceptible to cracking problems.

The comparison with other results, currently available in literature, has shown the effectiveness and the accuracy of this method. The value of this approach is to be found in its adaptability in analyzing membrane elements subjected to bending, shear, torsion and also combined loading. The results obtained from the analysis of the model are presented by means of graphs, from which the design data for crack-control, can be taken directly.

The curves are based on a tensile stress that can produce an average tensile deformation strain, which is adjusted with respect to a selected reference value.

The graphs are presented in a normalized form with respect to the strength of concrete and can be viewed as an effective and simple tool to aid a designer when addressing the problem of cracking.

Appendix A. Cracking diagrams (design charts)

Each graph in this Appendix shows, in a cartesian plane σ^*–τ^*, the normalized stresses ($\sigma^* = \sigma_l/f_c$; $\tau^* = \tau_{lt}/f_c$), for a fixed value of transverse to longitudinal reinforcement ratio $u = \rho_t/\rho_l$ and of the normalized deformation $\varepsilon_r/\varepsilon_0$, various curves (corresponding to different values of parameter k) where each one bounds with the axis of the abscissa a portion of the plane in which all the possible combinations of (σ^*, τ^*) can be found relative to stress conditions to which correspond fields of strains characterized by values of principal tensile strain which are less or equal to the predetermined limiting value. The graphs also show the inclination of the principal strains, which can be utilized to control the cracking angle. For example, according to the CEB-FIP Model Code [2], under the action of shear or torsion, the angle α must be limited to a range from 30° to 60° for better crack control.

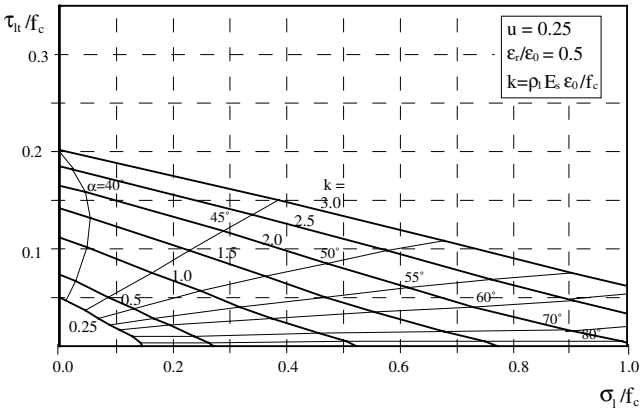

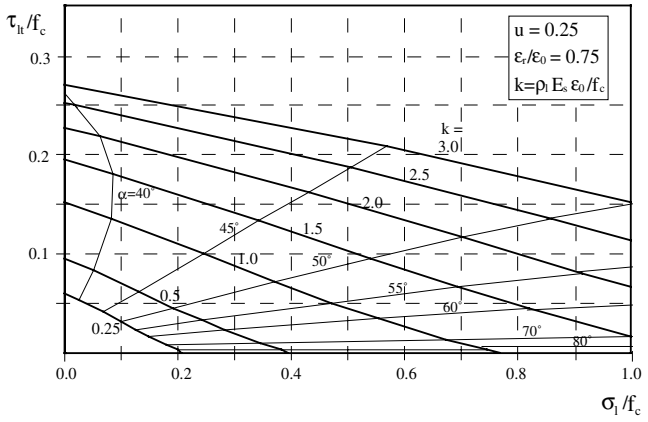

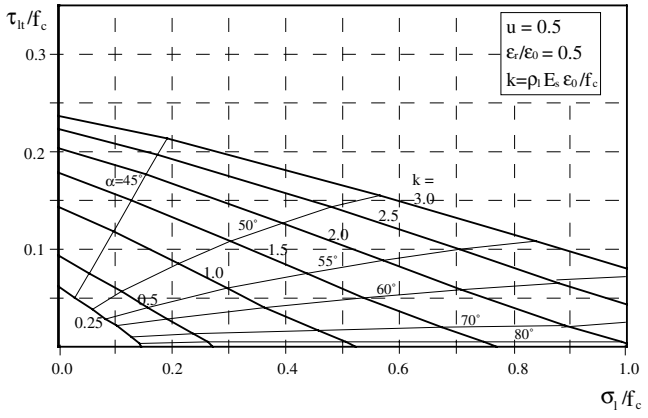

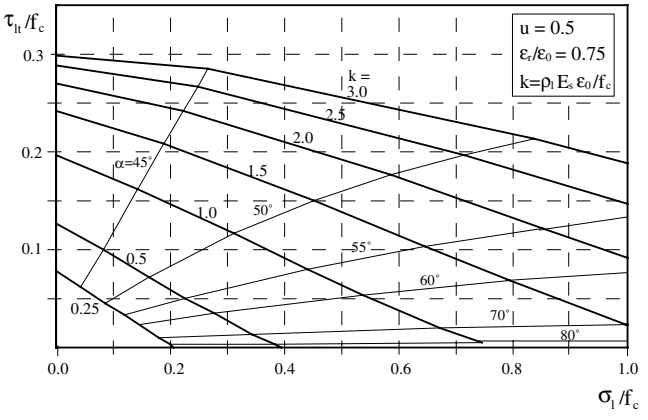

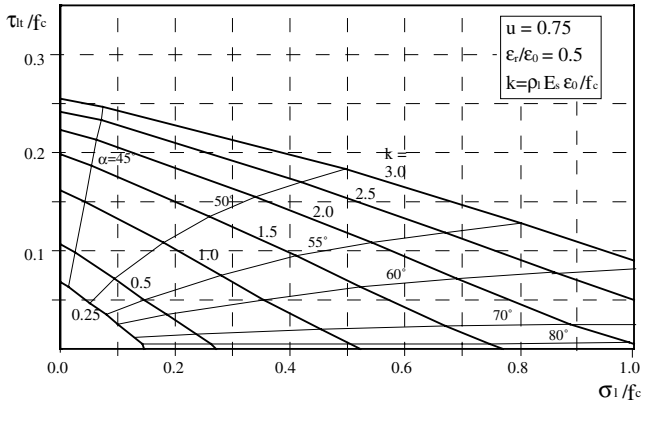

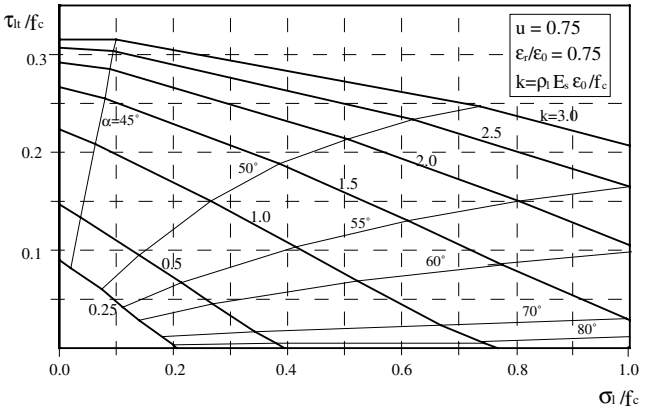

The interaction diagrams for crack-check in (RC) elements have been drawn for the following variables:

$u = \rho_t/\rho_l = 0.25;\ 0.50;\ 0.75$

$\varepsilon_r/\varepsilon_0 = 0.50;\ 0.75$

$k = \rho_l E_s \varepsilon_0/f_c = 0.25;\ 0.50;\ 1.00;\ 1.50;\ 2.00;\ 2.50;\ 3.00$

$\sigma_t/f_c = 0$

Appendix B. A numerical application

In the following, a numerical example to verify the crack-width in (RC) beams by means of the aforementioned graphs, is presented.

Given a simply supported (RC) beam, of rectangular section, with $L = 6000\,\text{mm}$ span length, $b = 300\,\text{mm}$ width, $h = 600\,\text{mm}$ height; $c = 35\,\text{mm}$ concrete cover; $6\phi18$ longitudinal steel rebars ($A_l = 1524\,\text{mm}^2$), $\phi10$ shear reinforcement at $s_t = 100\,\text{mm}$ c/c; C20/25 ($f_c = 20\,\text{MPa}$) concrete grade; S400 ($f_y = 400\,\text{MPa}$) steel reinforcement grade; uniformly distributed dead load of $G = 15\,\text{kN/m}$; uniformly distributed live load of $Q = 20\,\text{kN/m}$; maximum allowable crack-width of $w_a = 0.2\,\text{mm}$, under a frequent combined action (load combination factor $\psi_1 = 0.5$), verify the crack-width under service loads.

- *Half section ($x = L/2$)*

The forces acting on it are:

$$M = \frac{1}{8}(G + \psi_1 Q)L^2 = 112.5\ \text{kNm}; \quad V = 0$$

The distance x_c of the neutral axis for the partial section is given by

$$x_c = \frac{nA_l}{b}\left(-1 + \sqrt{1 + \frac{2bd}{nA_l}}\right) = 167\ \text{mm}$$

where $d = (h - c) = 565\,\text{mm}$, $n = E_s/E_c = 6.9$, having assumed that $E_s = 200\,\text{GPa}$, $E_c = 9.5(f_c + 8)^{1/3} = 28.8\,\text{GPa}$ (according to Eurocode 2 [6]).

Then from Eq. (19), the height of the membrane element can be determined:

$$h_m = \frac{(h - x_c)^3}{3(d - x_c)^2} = 171 \text{ mm}$$

The longitudinal steel ratio (assuming the steel area A_l can be concentrated over the entire section bh_m of the equivalent panel) and the transverse one are, respectively:

$$\rho_l = \frac{A_l}{bh_m} = 0.0297; \quad \rho_t = \frac{A_t}{bs} = 0.0052$$

and their ratio u is equal to:

$$u = \frac{\rho_t}{\rho_l} = 0.17$$

Furthermore, the value of parameter k is defined by Eq. (11)

$$k = \frac{\rho_l E_s \varepsilon_0}{f_c} = 0.59$$

having assumed that $\varepsilon_0 = 0.002$.

The parameter k allows us to locate the limit curve, below which the assumed tension stress is such as to permit that principal tensile strains (and corresponding crack-widths) are less than the limit value set in advance.

The tensile force acting on the membrane element of concrete is given by

$$T = \frac{M}{h^*} = 221 \text{ kN}$$

where $h^* = d - x_c/3 = 509$ mm is the internal lever arm.

Knowing the axial force T, the average longitudinal stress applied on the equivalent membrane element can be found:

$$\sigma_l = \frac{T}{bh_m} = 4.31 \text{ MPa}$$

while the average shear stress is obtained by

$$\tau_{lt} = \frac{V}{bh^*} = 0$$

The normalized values of stresses in the panel are:

$$\sigma^* = \frac{\sigma_l}{f_c} = 0.22; \quad \tau^* = \frac{\tau_{lt}}{f_c} = 0$$

The average principal tensile strain is the last parameter to be considered in order to select the appropriate graph.

Once the value of the design crack-width is fixed, it is possible to determine the average value through the coefficient $\beta_0 = 1.7$ [6]:

$$w_m = \frac{w_a}{\beta_0} = 0.1176 \text{ mm}$$

The average crack spacing is [Eq. (20)]:

$$s_{rm} = 50 + 0.25 k_1 k_2 \frac{\phi}{\rho_r} = 111 \text{ mm}$$

(having assumed that $\rho_r = A_l/bh_m = 0.0297$, $k_1 = 0.8$, $k_2 = 0.5$, $\phi = 18$ mm), from which the limit tensile strain is obtained:

$$\varepsilon_r = \frac{w_m}{s_{rm}} = 0.0011$$

A normalized value is obtained if ε_r is divided by the reference deformation ε_0:

$$\frac{\varepsilon_r}{\varepsilon_0} = 0.55$$

which is the last parameter necessary for the selection of the proper graph in order to obtain the corresponding crack value.

Using the graph with parameters $u = 0.25$, $\varepsilon_r/\varepsilon_0 = 0.5$ and locating a point whose coordinates are $\sigma^* = 0.22$, $\tau^* = 0$, through a linear interpolation, a value of k equal to 0.42 is found. The corresponding value of ρ_l is given by

$$\rho_l = \frac{k f_c}{E_s \varepsilon_0} = 0.021$$

This is the ratio of longitudinal rebars which can be considered the lowest percentage of reinforcement needed, in order to have an average tensile strain below the limit value set. Given that:

$$\rho_l(\text{needed}) = 0.021 < \rho_l(\text{available}) = 0.0297$$

it can seen that the crack check is satisfactory.

- *Quarter section ($x = L/4$)*

The values of forces acting at this position are:

$$M = (G + \psi_1 Q)\left(\frac{L^2}{8} - \frac{L^2}{32}\right) = 84.4 \text{ kNm};$$

$$V = (G + \psi_1 Q)\left(\frac{L}{2} - \frac{L}{4}\right) = 37.5 \text{ kN}$$

and solving as done previously:

$$T = \frac{M}{h^*} = 165.8 \text{ kN}; \quad \sigma^* = \frac{\sigma_l}{f_c} = \frac{T}{bh_m f_c} = 0.16;$$

$$\tau^* = \frac{\tau_{lt}}{f_c} = \frac{V}{bh^* f_c} = 0.0123$$

The average crack spacing is [Eq. (21)]:

$$s_{rm} = \frac{s_l + s_t}{2\sqrt{2}} = 75 \text{ mm}$$

having assumed $s_l = 50 + 0.25 k_1 k_2 \phi/\rho_r = 111$ mm (longitudinal rebars concentrated at the bottom level of the section), $s_t = 100$ mm. Operating as previously, it follows that:

$$\varepsilon_r = \frac{w_m}{s_{rm}} = 0.0016; \quad \frac{\varepsilon_r}{\varepsilon_0} = 0.8; \quad u = \frac{\rho_t}{\rho_l} = 0.17$$

From the table with parameters $u = 0.25$, $\varepsilon_r/\varepsilon_0 = 0.75$, and considering a point whose coordinates are $\sigma^* = 0.16$, $\tau^* = 0.0123$, a value of k equal to 0.25 is obtained, to which the ratio of longitudinal reinforcement $\rho_l = kf_c/E_s\ \varepsilon_0 = 0.0125$ corresponds. Given that:

$$\rho_l(\text{needed}) = 0.0125 < \rho_l(\text{available}) = 0.0297$$

even for this section the crack-check is quite satisfactory.

References

[1] Braam CR, Walraven JC. Control of crack width in deep reinforced concrete beams. IABSE Colloquium Structural Concrete, Stuttgart, IABSE-report, V.62, 1991, 111–116.

[2] CEB-FIP. Model code for concrete structures. CEB-FIP International Recommendation, Comitè Euro-International du Beton, 1990.

[3] CEB. Cracking and deformation. Bulletin d'Information N.158, Comitè Euro-International du Beton, 1985.

[4] Colotti V. Nonlinear analysis of reinforced concrete panels. In: Procs. Giornate AICAP, Italian Association of Reinforced and Prestressed Concr. Struct., Spoleto, Italy (in Italian), 1991, p. 81–96.

[5] Desayi P, Rao KB. Probabilistic analysis of the cracking of RC beams. Mater Struct, RILEM 1987;20(120):408–17.

[6] Eurocode 2. Design of concrete structures, part 1, general rules and rules for buildings. CEN, European Committee for Standardization, Bruxelles, 1991.

[7] Frosch RJ. Another look at cracking and crack control in reinforced concrete. ACI Struct J 1999;96(3):437–42.

[8] Hsu TTC. Unified theory of reinforced concrete. Boca Raton, Florida, USA: CRC Press Inc.; 1993.

[9] Hsu TTC. ACI shear and torsion provisions for prestressed hollow girders. ACI Struct J 1997;94(6):787–99.

[10] Iori I, Dei Poli S. Sulla torsione di elementi strutturali in cemento armato. L'Industria Italiana del Cemento 1985(2):121–9 (in Italian).

[11] Leonhardt F. Crack control in conctrete structures. Zurich: IABSE Surveys; 1977. S-4/77.

[12] Makhlouf HM, Malhas FA. The effect of thick concrete cover on the maximum flexural crack width under service load. ACI Struct J 1996;93(3):257–65.

[13] Oh BH, Kang YJ. New formulas for maximum crack width and crack spacing in reinforced concrete flexural members. ACI Struct J 1987;84:103–12. March–April.

[14] Rahal KN, Collins MP. Effect of thickness of concrete cover on shear-torsion interaction—an experimental investigation. ACI Struct J 1995;92(3):334–42.

[15] Rasmussen LJ, Baker G. Torsion in reinforced normal and high-strength concrete beams—part 1: experimental test series. ACI Struct J 1995;92(1):56–62.

[16] Tan KH, Mansur MA, Huang LM. Reinforced concrete t-beams with large web opening in positive and negative moment regions. ACI Struct J 1996;93(3):277–89.

[17] Wiche M. Cracking and deformation in structural concrete. IABSE Colloquium Structural Concrete, Stuttgart, IABSE-report, V.62, 1991, 49–57.

[18] Yoon YS, Cook WD, Mitchell D. Minimum shear reinforcement in normal, medium, and high-strength concrete beams. ACI Struct J 1996;93(5):576–84.